

# The relationship between the structural anisotropy of the PFA polymer/compressed expanded graphite-matrix composites and acoustic emission characteristics

Sylwia BERDOWSKA<sup>1</sup>, Janusz BERDOWSKI<sup>1,2\*</sup>, and Frederic AUBRY<sup>3</sup>

<sup>1</sup> Faculty of Electrical Engineering, Czestochowa University of Technology, Al. Armii Krajowej 17, 42-200 Czestochowa, Poland

<sup>2</sup> Faculty of Science and Technology, J. Dlugosz University in Czestochowa, Al. Armii Krajowej 13/15, 42-200 Czestochowa, Poland

<sup>3</sup> Maitrise de Chimie-Physique, Université Henri Poincaré, Nancy, France

**Abstract.** The main aim of the study was to search for the relationship between the anisotropy of the structure of polyfurfuryl alcohol (PFA) – polymer/compressed expanded graphite (CEG)-matrix composites at subsequent stages of the technological process and characteristics of the acoustic emission (AE) descriptors. These composites, obtained after successive technological procedures of impregnation, polymerization, and carbonization, possess different structure, densities, porosity, and other physicochemical properties. In the structures of composites prepared on the basis of CEG, two basic directions can be distinguished: parallel to the bedding plane of graphite sheets and perpendicular to it. The measurements were carried out for the stress acting in these two main directions. The investigation has shown that the AE method enables the detection of anisotropy in the structure of materials. The results of the research show that all four of the acoustic emission descriptors studied in this work are sensitive to the technological stages of these materials on the one hand and their structure anisotropy on the other. Fourier analysis of the recorded spectra provides interesting conclusions about the structural properties of composites as well as a lot of information about the bonding forces between the carbon atoms of which the CEG matrix is composed and the PFA polymer or turbostratic carbon.

**Key words:** acoustic emission; spectrum distribution; anisotropic structure; polyfurfuryl alcohol; compressed expanded graphite; composite membrane.

## 1. INTRODUCTION

The basic material for all composites produced in our work was compressed expanded graphite (CEG). It is a layered material made of 10 nm thickness graphite flakes. The structure, anisotropy, and porosity of the CEG depend on the manufacturing technology. Previous studies [1–5] showed that the pore sizes vary from about 1 nm up to 100 μm and molecular chains of different polymers intercalated into the open pores of CEG [6, 7]. This process is caused by the adsorption mechanisms, high pore density, and appropriate pore shapes. For these reasons, CEG is a good matrix for making different kinds of polymer/carbon materials.

Polyfurfuryl alcohol (PFA) is largely used in chemistry due to its excellent thermal stability, remarkable resistance to acidic conditions, as well as to degradation caused by fire and corrosion [8]. It should be emphasized that PFA produces a high carbon yield if it undergoes pyrolysis [9]. For this reason, PFA is a good precursor to produce nanostructured carbon materials and carbon-based nanocomposites for applications such as molecular sieve adsorbents and electrodes [10, 11]. PFA can be

also polymerized in situ to create special types of membranes that resist acid [12] or for fuel cell applications [13].

The main aim of the study in the frame of this work was to analyze the relationship between the structure of the compressed expanded graphite matrix – PFA polymer – turbostratic carbon composites on successive stages of technological process and characteristics of parameters describing the acoustic emission (AE) phenomena in these materials. After subsequent technological stages, these composites, whose general formula can be written as PFA/CEG, are characterized by a different structure, density, porosity, and many other physicochemical properties. The anisotropy of the structures of the CEG matrix and the composites based on it has not been investigated by the AE method so far.

Due to the very wide potential practical applications of the PFA composites, for example as catalysts [14, 15], gas separation membranes [16–18], or proton exchange membranes in fuel cells [19–22], it is important to study their different properties.

## 2. PREPARATION OF COMPOSITES

In the present work, the PFA-polymer/CEG-based composites were obtained by PFA vacuum impregnation into a CEG matrix of different densities. The technology of producing composites of this type is presented in our paper [23]. The raw EG flakes

\*e-mail: j.berdowski@ujd.edu.pl

Manuscript submitted 2021-03-18, revised 2021-05-05, initially accepted for publication 2021-05-10, published in October 2021

were first compressed into rectangular graphite blocks with densities ranging from 90 to 130 mg/cm<sup>3</sup>, respectively. This range was chosen because previous experiments had shown that a density of about 110 mg/cm<sup>3</sup> was most suitable for chemical treatment [23, 24].

The composite preparation diagram for all stages of the technological process is shown in Fig. 1. Starting with a graphite crystal, the CEG matrix is produced and the PFA-polymer/CEG-matrix composites are obtained through subsequent chemical and physical processes. The final material consists of a CEG matrix and polymerized and carbonized PFA – it is turbostratic carbon, which fills up the open pores. It should be emphasized that the individual composites shown in Fig. 1 have various and important applications. Three materials from this diagram were selected for research. Successively, they were CEG matrix with a homogeneous, anisotropic, and very porous structure; POL composite made of CEG after vacuum impregnated and polymerized PFA processes; CAR composite produced on the basis of POL after the high-temperature carbonization process with a heterogeneous, anisotropic structure.

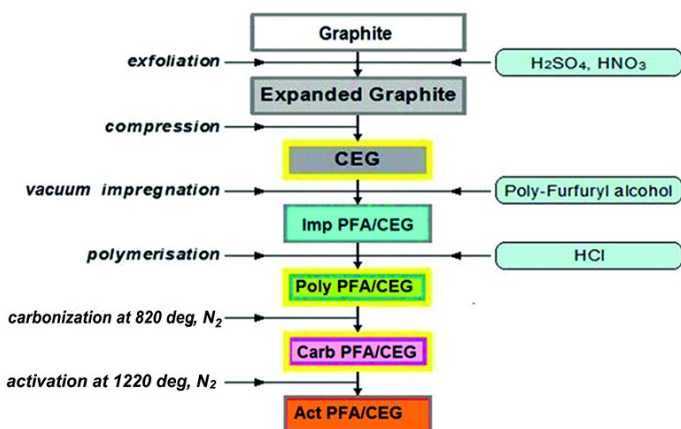


**Fig. 1.** Schematic diagram of technological procedures of the PFA-polymer/CEG-matrix composites

### 3. MICROSTRUCTURE OF THE COMPOSITES

The structure of composites is built of graphite sheets constituting the matrix and a polymerized or carbonized material, which fills up the open macropores. The bedding planes of graphite flakes are approximately parallel to each other; for this reason, the structure of the composite is anisotropic. There are strong bonds between carbon atoms in the plane of the crystalline graphite layer in the form of delocalized  $\pi$  orbitals, whereas between the carbon layers there occur only weak Van der Waals forces [4]. These properties are extremely important due to the method of acoustic emissions used in our research.

During vacuum impregnation, the PFA resin penetrates the open pores of the CEG matrix. Impregnation does not change the elementary component of the CEG structure, which is formed by the texture of the stacked graphite layers. However, PFA impregnation into the matrix changes the pore structure in the CEG. The anisotropy of the composite structure is increasing as the density of the crude CEG matrix increases, which has been experimentally confirmed. For the group of composites produced on the CEG matrices with lower density – below 260 mg/cm<sup>3</sup>, their porosity, pore diameter, and specific pore, volume decreased abruptly after PFA impregnation. In the case of the CEG matrix with even higher initial densities, the anisotropy of the composites has become more visible. It can be explained by the increasing number of evenly spaced graphite layers in the composite structure. The conclusion is that after the technological processes the composites retain the internal structure of the CEG sheets and the impregnation with PFA resin does not destroy this microstructure.

Figure 2 shows the morphology of CEG blocks and PFA/CEG composite samples obtained from micrographs. The optical microscope used to study the structure of the samples was an Axioskop MPM 200, Carl Zeiss. In three microphotographs (Fig. 2 – level 1), a change in the texture of composites is visible after individual technological processes, in the plane perpendicular to the layered structure. Changes in their structure and porosity are visible. These pictures show the differences between the CEG matrix structure and the polymerized or carbonized state

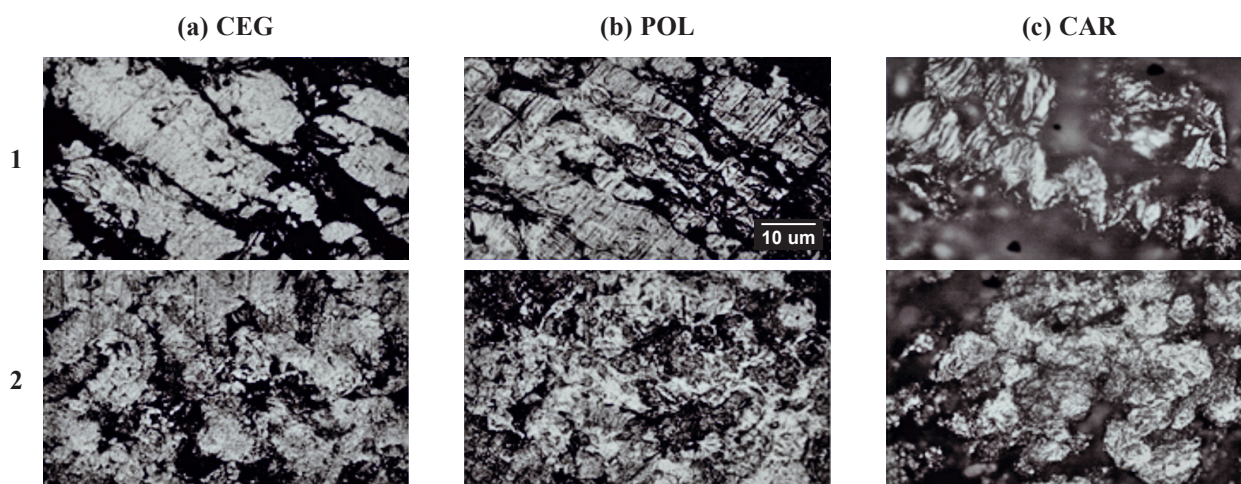


**Fig. 2.** Microstructures of the composites, 1 – cross-section to the bedding plane, 2 – parallel to the bedding plane (a) CEG  $d = 260$  mg/cm<sup>3</sup>, b) POL  $d = 669$  mg/cm<sup>3</sup>, c) CAR  $d = 428$  mg/cm<sup>3</sup>

of the materials. The layered structure of the CEG matrix is still observable in the POL and CAR composites also after the pyrolysis procedure. Figure 2 – level 2 shows changes in the texture of the investigated composites in the plane parallel to the layered structure at each stage of the technological process. The comparison of levels 1 and 2 in Fig. 2 also shows the anisotropy and differences in the layered structure of the CEG matrix and the produced PFA/CEG composites appearing in two main planes.

#### 4. ACOUSTIC EMISSION CHARACTERISTICS IN PFA/CEG COMPOSITES FOR THE MAIN PLANES OF THE STRUCTURE

The acoustic emission resulting from the applied pressure can be used to measure the changes in the structure and many different material properties [25–28]. The study of AE phenomena in composites after each stage of the technological process, i.e., impregnation, polymerization, and carbonization allow us to analyze the influence of modification in the chemical composition on the change of individual AE descriptors. The results of these studies have been partially presented in our previous works [23, 24]. This paper presents the results of investigations on changes in AE parameters depending on the location of the stress plane in the structure, which were analyzed in different groups of composites.

##### 4.1. Method of acoustic emission measurements

In this work, modern AE methods were used to investigate the structure anisotropy as well as many other physical and chemical properties of composites. The measurements of AE characteristics in PFA/CEG composites described in Part 2 were performed using the following equipment: AE Analyzer model EA-100NEURAL, Institute FTR PAS, Poland, and Materials Testing Machine model LRX, Lloyd Instr. England. The AE descriptors were tested in a wide frequency range of acoustic waves (0.1–2.5 MHz), using a piezoelectric sensor type SE2MEG-P, Dunegan Eng. Cons. Inc. USA. A detailed description of the experimental arrangement and the AE parameters measurement procedure are presented in our paper [23]. As the AE waves were recorded and analyzed using computer techniques, it was possible to determine more AE descriptors in one experiment, which facilitated the analysis of many different properties of the tested composites [29–31]. Among the many registered parameters characterizing AE signals, four of them (the sum of counts, the sum of events, the  $W_{ce}$  ratio, and the spectrum distribution of acoustic waves) were selected for analysis in this work.

At the stage of preparing the CEG texture, a graphite matrix with a strong asymmetry was produced. In the structures of composites prepared on the basis of CEG-matrix, two basic directions can be distinguished: perpendicular to the layer planes of graphite sheets and parallel to it, as shown in Fig. 3. All the results presented in the paper were obtained for uniaxial stress applied in these two main directions. It should be noted that due to the very low stiffness of the CEG matrix, AE measurements in the perpendicular geometry were not possible to be performed in a raw CEG. The results of the research on AE characteristics for various types of PFA/CEG structures are presented in the following sections.

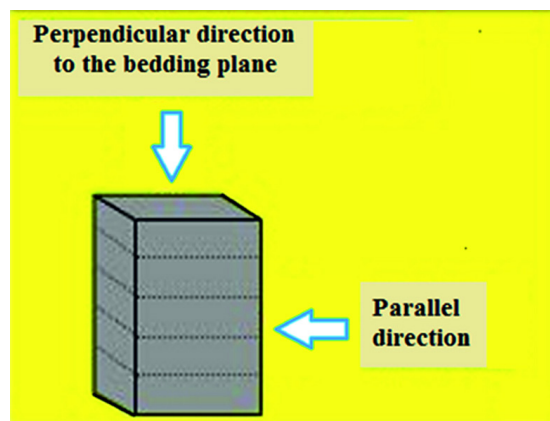
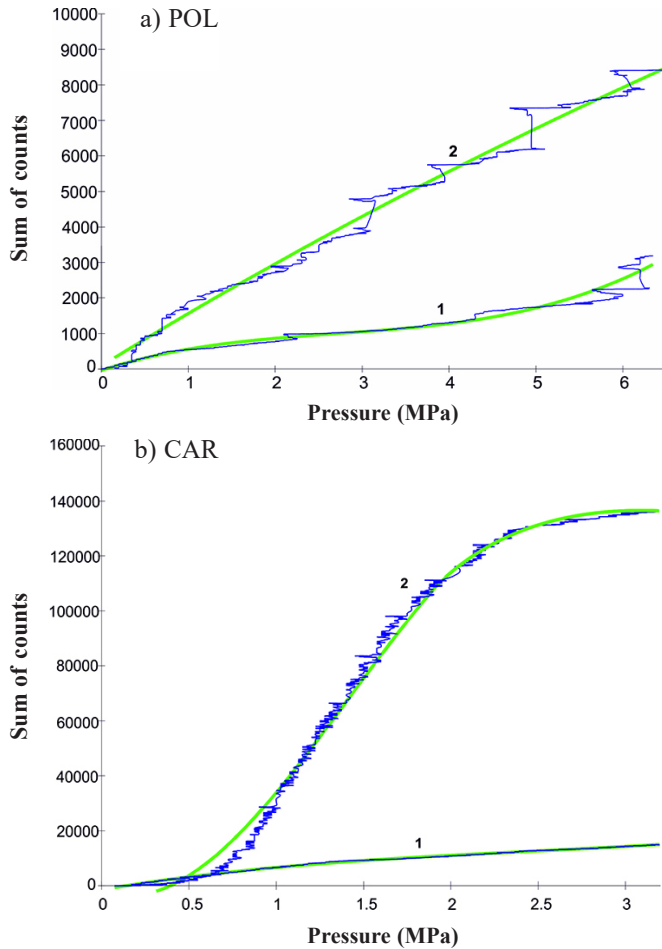


Fig. 3. Main directions in the layered structure of composites

##### 4.2. The relationship between the composite structure anisotropy and the sum of counts or the sum of events AE pulses

The results of the research on the AE descriptor, which is the sum of counts of the pulses in POL and CAR materials for the compression stress applied in two main directions parallel or perpendicular to the bedding plane of the structure, are compared in Fig. 4. The results of investigations for the second parameter, which is the sum of events in POL and CAR structures for stress applied in both main planes of the layered structure are compiled in Fig. 5. The comparison and analysis of the sum of counts and sum of events in these composites led to the following conclusions. For both AE descriptors, the largest values were measured in the CAR structure. Both are more than ten times greater in CAR than for POL composites. The obtained results confirm the highest acoustic emission activity in CAR composite. After analyzing the measurement results concerning the acoustic activity of the studied groups of materials, it was concluded that they can be directly related to their elastic properties. Namely, the CEG matrix has the properties of a soft and brittle material. On the other hand, after the PFA impregnation and polymerization processes, it is transformed into POL material – heterostructural with less anisotropy, which is both hard and flexible. After the next carbonization process, the anisotropy of the layered structure of the composite increased and it has the properties of hard and brittle material at the same time. As measured in previous studies [23], the compressive strength for the pressure applied in the bedding plane in the POL composite is about 12 MPa, while in CAR material it is about 4 MPa.

On the other hand, the comparison of the sum of counts or sum of events for the same group of composites, but in both main planes of the layered structure, gives conclusions on the anisotropy of their structure. Comparing these AE characteristics in two main planes of the structure, it was shown that in both POL and CAR composites, the acoustic activity is much higher when the measurements were carried out for the stress acting in the direction perpendicular to the bedding plane and they were about 3 times higher in POL and about 10 times higher in CAR. These measurement results can be



**Fig. 4.** Sum of counts vs. pressure applied in the direction parallel – 1 or perpendicular – 2 to the bedding plane for a) POL ( $d = 660 \text{ mg/cm}^3$ ); and b) CAR ( $d = 498 \text{ mg/cm}^3$ ) composites. Results of measurements – navy-blue curve, polynomial fitting – green line

explained based on the microstructure of the PFA/CEG-matrix composites presented in Section 3. CEG matrix is a layered material, and there are strong bonds between carbon atoms in the plane of the crystalline graphite in the form of delocalized  $\pi$  orbitals, whereas between the carbon layers there occur only weak Van der Waals type forces. After the technological processes, the composites retain the internal structure of the CEG in the form of layered graphite sheets. For these reasons, for the stress applied in the direction perpendicular to the plane of the graphite sheets, there are many compressive cracks in the structure and the acoustic activity of the composites is much higher. Whereas for the stress applied in the direction parallel to the layers of structure there is a small number of shear cracks and the slip of graphite planes, and the acoustic activity of composites is low. The obtained results are extremely important and interesting as they show direct relationships between the structural anisotropy of PFA polymer/compressed expanded graphite-based composites and AE descriptors. It can also be concluded from them that the structural anisotropy of POL composites is much smaller than that of materials after the carbonization process (Figs. 4 and 5). This phenomenon can be

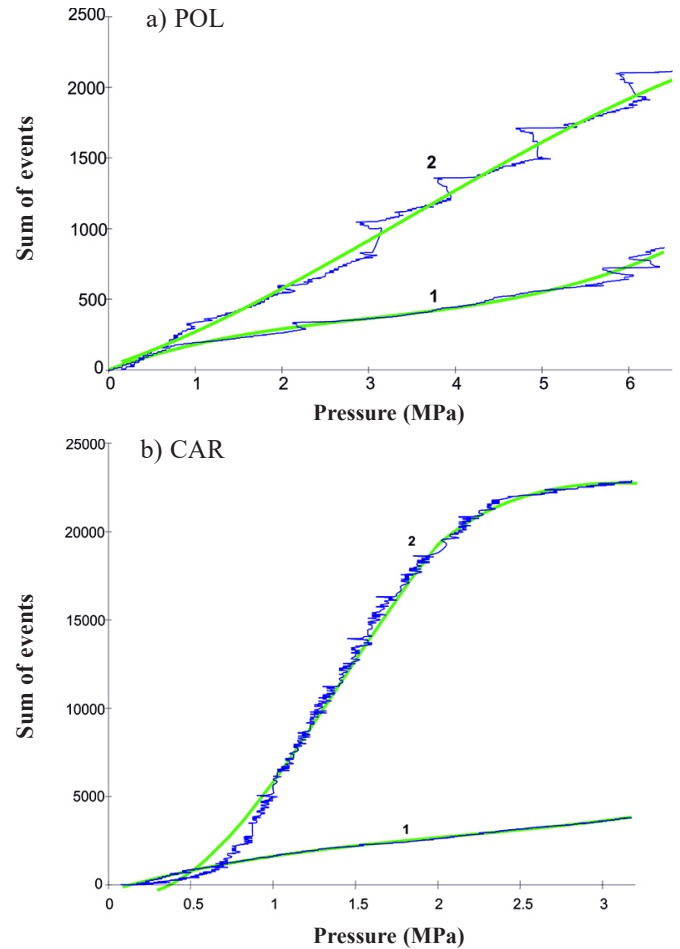


**Fig. 5.** Dependence of sum of events on pressure applied in the direction parallel – 1 or perpendicular – 2 to the layered structure a) POL ( $d = 660 \text{ mg/cm}^3$ ); and b) CAR ( $d = 498 \text{ mg/cm}^3$ ) composites. Results of measurements – navy-blue curve, polynomial fitting – green line

explained based on the changes in the structure and chemical composition of the materials presented in Section 3. Generally, it can be stated that the difference in the values of these AE descriptors determined in the two main planes is a measure of the composite structure anisotropy.

The formula  $W_{ce} = \Sigma N_{cnt} / \Sigma N_{ev}$  defines the third AE descriptor. The value of this parameter varies depending on the type of material and the location of the measurement plane in the structure. Moreover, its value is directly related to the average frequency of generated acoustic pulses and their duration [32]. It was found in the obtained results that the minimum value of the  $W_{ce}$  descriptor was reached in CEG, the average in POL, and the maximum in CAR materials. From these results, it can be concluded that the transition on higher levels after technological processes was reflected in the rapid increase in the frequency of the emitted elastic waves. Figures 6 and 7 show the results of the analysis of  $W_{ce}$  descriptor changes as a function of composite density. The results in the POL and CAR composites were obtained for the stresses applied in both main directions of the structure. The performed research proved that this descriptor is dependent on its density for all compos-

The relationship between the structural anisotropy of the PFA polymer/compressed expanded graphite-matrix composites and acoustic emission...

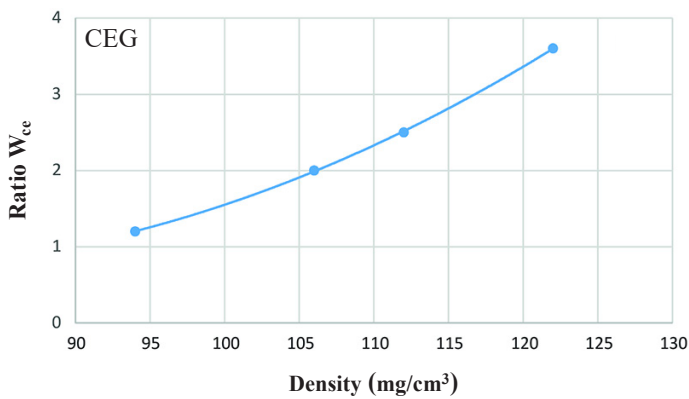


**Fig. 6.**  $W_{ce}$  ratio depending on the density of CEG, pressure applied in the direction parallel to the layered structure

ites. The dependence of  $W_{ce}$  on the asymmetry of the composite structure is also visible.

#### 4.3. Analysis of the spectrum distribution of AE waves depending on the anisotropy of the composite structure

In order to obtain the spectral distribution of the elastic waves generated in the materials, the frequency analysis of the recorded AE signals was performed using the Fourier transformation [25, 33–35]. Figure 8 presents a summary of the research results of the frequency spectrum of the generated acoustic waves in individual structures. The measurements were performed for two directions of the applied stress: parallel or perpendicular to the layered structure.

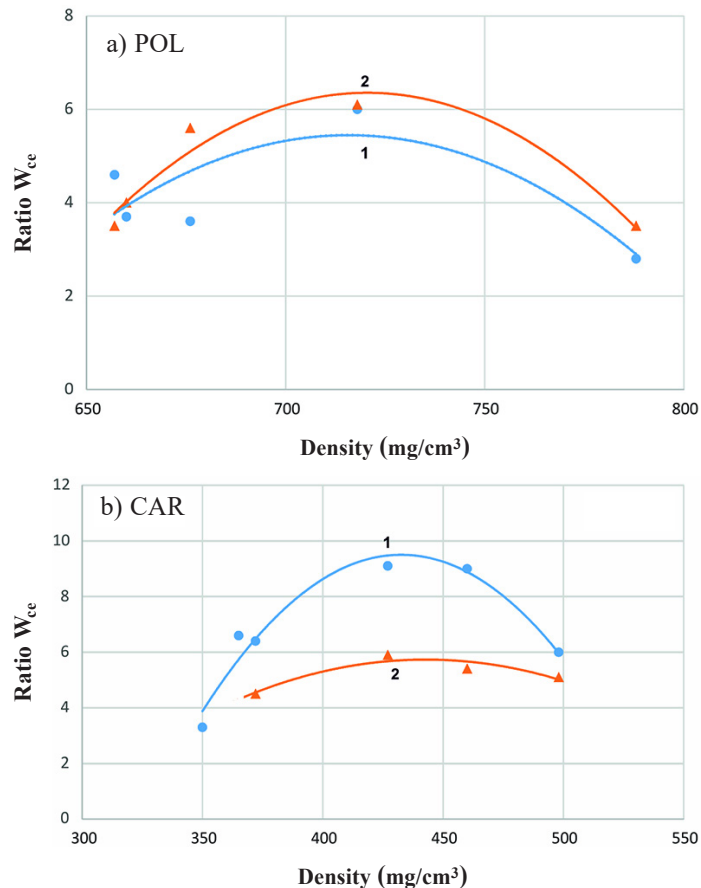


**Fig. 7.** The  $W_{ce}$  ratio vs densities of a) POL; b) CAR composite, pressure applied in the direction parallel – 1 or perpendicular – 2 to the bedding plane

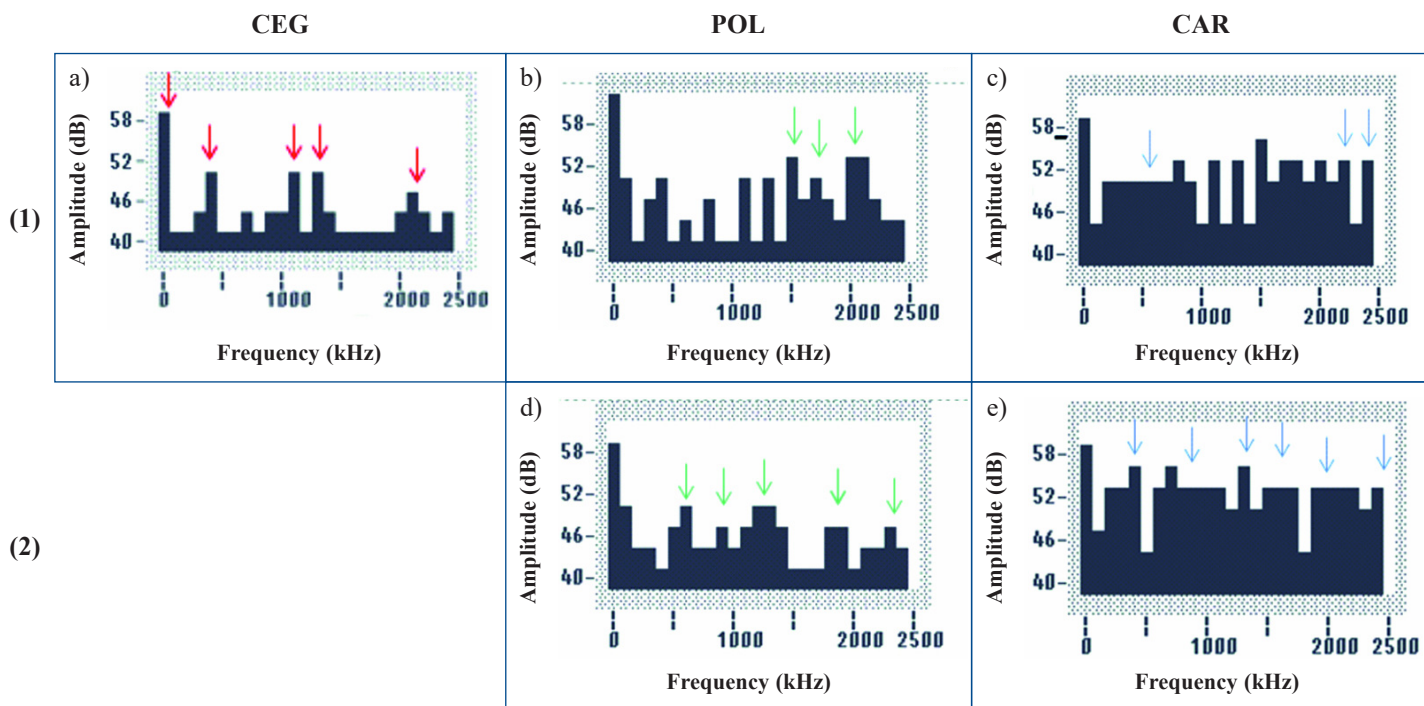


**Fig. 8.** Fourier analysis of the frequency spectrum of elastic waves for a) CEG  $d = 107 \text{ mg/cm}^3$ ; b) and d) POL  $d = 660 \text{ mg/cm}^3$ ; c) and e) CAR  $d = 498 \text{ mg/cm}^3$  composites, pressure applied in the direction parallel (1) or perpendicular (2) to the layered structure

Figure 8a shows the spectral distribution measured in the CEG material for the stress in the parallel plane. Five red arrows denote 5 frequency bands of the emitted elastic waves, which are also repeated in the spectra of POL and CAR structures. These observations show an extremely interesting conclusion that the stress in parallel planes in the CEG structure generates elastic pulses of the same frequency and approximate intensity as in the heterogeneous POL and CAR materials. The repetition of these bands is clearly visible in Figs. 8b and 8c. These observations indicate that the composites essentially retain the internal structure of the CEG sheets.

Figure 8b shows the frequency spectrum of the elastic waves recorded in the POL material. The measurements were carried out for the stress acting in the plane of the layered structure. The analysis of this spectrum showed that three frequency bands appeared on it, which were also observed in the CAR structure, but not in the CEG spectrum. The green arrows indicate these three bands in the diagram. Figure 8c shows the measured spectral distribution of the acoustic pulses in the CAR material, for the stress applied in the parallel plane. The blue arrows indicate three particular wave frequency bands that are only found in the spectrum of this type of composite. Such dominant frequency bands were not observed in the other two types of materials.

The presented results of the spectral analysis are fully consistent with the results presented in Subsection 4.2, in which the analysis of the frequency increase of the generated elastic waves for PFA/CEG composites after subsequent technological processes was shown based on other AE descriptors. The increase in the frequency of individual peaks in the spectra is generally associated with a reduction in the size of the sources generating the acoustic waves [32]. The results of research on spectral distributions performed in POL and CAR composites when the measurements were carried out for stress acting perpendicularly to the layered structure are shown similarly in Figs. 8d and 8e.

The above-mentioned specific frequencies of the bands of the emitted elastic waves in the studied types of materials and for both main planes of the structure are compiled in Table 1. The study of the presented spectral distributions for parallel geometry indicated that the impregnation of the PFA resin into the CEG precursor and its polymerization causes a significant increase in the frequency of the peaks. After the next process of carbonization of the POL material, a further increase in the frequency of the bands was observed. Two intense bands with frequencies above 2 MHz have emerged in the CAR composite.

The comparison of spectral distributions for the same group of composites in both main planes of the layered structure allows us to draw conclusions about the anisotropy of their internal structure. Such an analysis performed for the two main planes of the structure shows that intense wide bands appear in the spectrum in the entire studied frequency range both in POL and CAR composites for the stress applied in the perpendicular direction. In contrast, in the case of parallel geometry in these materials, completely different spectral distributions of frequency were obtained with a predominance of peaks in the upper bands of the investigated range.

**Table 1**

The specific frequencies of the bands of acoustic pulses in various types of materials for the main planes of the structure

Material	Density [mg/cm <sup>3</sup> ]	Frequency bands parallel plane [MHz]	Frequency bands perpendicular plane [MHz]
CEG	112	0.1 0.4 1.1 1.3 2.1	
POL PFA/CEG	660	0.8 1.5–1.8 2.0–2.2	0.6 0.9 1.1–1.4 1.8–1.9 2.3
CAR PFA/CEG	498	0.2–0.9 2.2 2.4	0.2–0.4 0.6–1.2 1.4 1.5–1.8 1.9–2.3 2.5

## 5. CONCLUSIONS

Based on the results of research on AE phenomena carried out in porous PFA polymer/CEG-matrix composites with a layered structure at individual stages of their technological process of impregnation, polymerization, and carbonization, the following conclusions were formulated:

- The research has shown that the AE method enables the detection of anisotropy in the structure of materials. The results of the research showed that all four of the acoustic emission descriptors studied in this work are sensitive to the technological stages of these materials on the one hand and their structural anisotropy on the other. By comparing the changes of all studied AE descriptors for both main planes of the structure, it was assessed that the most sensitive to anisotropy changes are the sum of counts and the sum of events. The difference in the values of these descriptors, determined for the two main planes, is a measure of the composite structure anisotropy.
- The largest magnitude of the AE parameters, the sum of counts and the sum of the events, was measured in CAR materials for both main planes of the composite structure. It can be concluded that the CAR composites showed the highest acoustic activity among all the tested materials. Such high activity in generating elastic waves is shown by materials with hard and brittle mechanical properties and a porous structure. It was also found that the acoustic activity is much greater for the stresses applied in the direction perpendicular to the bedding plane in both POL and CAR composites than for the parallel direction.
- From the measurements of these two descriptors, it can also be concluded that the structural anisotropy of POL

composites is much smaller than that of materials after the carbonization process. Due to the anisotropy of the CEG matrix precursor, the PFA/CEG composites obtained after the technological processes had an anisotropic structure. PFA impregnation into the graphite matrix reduced the anisotropic structure by introducing an amorphous component and changed the pore structure. However, it did not change the elementary structure component, which was formed by uniformly oriented graphite layers. This explains the anisotropy observed in individual groups of composites and its reduction after impregnation.

- The performed research proved that value of the  $W_{ce}$  descriptor changes with the density of composites. The dependence of this descriptor on the asymmetry of the composite structure has also been shown.
- A comparison of the AE waves spectrum distributions between different composites (CEG, POL, and CAR) for the stress in the parallel plane showed that they are different, but some frequency bands are repeated. These observations indicate that the composites essentially retain the internal structure of the graphite flakes. The layered structure derived from the CEG matrix, as well as the shape and size of the pores explain the structure anisotropy of all tested composites.
- The research confirmed that the impregnation of the PFA resin into the CEG precursor and its polymerization causes a significant increase in the frequency of the peaks for parallel geometry of measurements. After the next process of carbonization of the POL material, a further increase in the frequency of the bands was observed. These phenomena generally indicate a reduction in the size of the sources emitting acoustic waves.
- The comparison of the spectral characteristics in the two main planes of the structure shows that both in the POL and CAR composites for stress in the perpendicular direction, intense wide bands appear in the spectrum in the entire studied frequency range. In contrast, in the case of parallel geometry in these materials, a completely different spectrum distribution of frequency was obtained with a predominance of peaks in the upper bands of the investigated range. Fourier analysis of the recorded spectra provides very interesting conclusions about the structural properties of composites as well as a lot of information about the bonding forces between the carbon atoms of which the graphite matrix and the PFA polymer are composed.

## REFERENCES

- [1] A. Celzard, M. Krzesinska, D. Begin, J. Mareche, S. Puricelli, and G. Furdin, "Preparation, electrical and elastic properties of new anisotropic expanded graphite-based composites", *Carbon*, vol. 40, pp. 557–566, 2002, doi: [10.1016/S0008-6223\(01\)00140-3](https://doi.org/10.1016/S0008-6223(01)00140-3).
- [2] L. Shi, Z. Li, W. Yang, M. Yang, Q. Zhou, and R. Huang, "Properties and microstructure of expandable graphite particles pulverized with an ultra-high-speed mixer", *Powder Technol.*, vol. 170, no. 3, pp. 178–184, 2006.
- [3] W. Zheng, and S. Wong, "Electrical conductivity and dielectric properties of PMMA/expanded graphite composites", *Compos. Sci. Technol.*, vol. 63, pp. 225–235, 2003.
- [4] J. Fu, H. Xu, Y. Wu, Y. Shen, and Ch. Du, "Electrical properties and microstructure of vinyl ester resin/compressed expanded graphite-based composites", *J. Reinf. Plast. Compos.*, vol. 31, pp. 3–11, 2012, doi: [10.1177/0731684411431355](https://doi.org/10.1177/0731684411431355).
- [5] E. Solfitia and F. Bertoa, "A review on thermophysical properties of flexible graphite". *Procedia Struct. Integrity*, vol. 26, pp. 187–198, 2020. doi: [10.1016/j.prostr.2020.06.022](https://doi.org/10.1016/j.prostr.2020.06.022).
- [6] F. Uhl, Q. Yao, H. Nakajima, E. Manias, and Ch. Wilkie, "Expandable graphite/polyamide-6 nanocomposites", *Polym. Degrad. Stabil.*, vol. 89, pp. 70–84, 2005.
- [7] P. Xiao, M. Xiao, and K. Gong, "Preparation of exfoliated graphite/polystyrene composite by polymerization-filling technique", *Polymer*, vol. 42, pp. 4813–4816, 2001.
- [8] G. Nanni *et al.*, "Poly(furfuryl alcohol)-Polycaprolactone blends", *Polymers*, vol. 11, pp. 1069–1982, 2019, doi: [10.3390/polym11061069](https://doi.org/10.3390/polym11061069).
- [9] H. Wang and J. Yao, "Use of Poly(furfuryl alcohol) in the fabrication of nanostructured carbons and nanocomposites", *Ind. Eng. Chem. Res.*, vol. 45, pp. 6393–6404, 2006.
- [10] C. Burket, R. Rajagopalan, A. Marencic, K. Dronvajjala, and H. Foley, "Genesis of porosity in polyfurfuryl alcohol derived nanoporous carbon", *Carbon*, vol. 44, pp. 2957–2963, 2006.
- [11] L. Pranger, G. Nunnery, and R. Tannenbaum, "Mechanism of the nanoparticle-catalyzed polymerization of furfuryl alcohol and the thermal and mechanical properties of the resulting nanocomposites", *Compos. Part B Eng.*, vol. 43, pp. 1139–1146, 2012. doi: [10.1016/j.compositesb.2011.08.010](https://doi.org/10.1016/j.compositesb.2011.08.010).
- [12] C. Guo, L. Zhou, and J. Lv, "Effects of expandable graphite and modified ammonium polyphosphate on the flame-retardant and mechanical properties of wood flour-polypropylene composites", *Polym. Compos.*, vol. 21, pp. 449–456, 2013.
- [13] L. Jin, W. Huanting, C. Shaoan, and C. Kwong-Yu, "Nafion-polyfurfuryl alcohol nanocomposite membranes for direct methanol fuel cells", *J. Memb. Sci.*, vol. 246, pp. 95–101, 2005.
- [14] W. Li, Ch. Han, W. Liu, M. Zhang, and K. Tao, "Expanded graphite applied in the catalytic process as a catalyst support", *Catal. Today*, vol. 125, no. 3–4, pp. 278–281, 2007, doi: [10.1016/j.cattod.2007.01.035](https://doi.org/10.1016/j.cattod.2007.01.035).
- [15] A. Celzard, J. Mareche, and G. Furdin, "Modeling of exfoliated graphite", *Prog. Mater. Sci.*, vol. 50, pp. 93–179, 2005.
- [16] M.B. Shiflett and H.C. Foley, "Ultrasonic deposition of high-selectivity nanoporous carbon membranes", *Science*, vol. 285, pp. 1902–1905, 1999, doi: [10.1126/science.285.5435.1902](https://doi.org/10.1126/science.285.5435.1902).
- [17] M.B. Shiflett and H.C. Foley, "On the preparation of supported nanoporous carbon membranes", *J. Membr. Sci.*, vol. 179, pp. 275–282, 2000, doi: [10.1016/S0376-7388\(00\)00513-5](https://doi.org/10.1016/S0376-7388(00)00513-5).
- [18] C. Song, T. Wang, X. Wang, J. Qiu, and Y. Cao, "Preparation and gas separation properties of poly(furfuryl alcohol)-based C/CMS composite membranes", *Sep. Purif. Technol.*, vol. 58, pp. 412–418, 2008, doi: [10.1016/j.seppur.2007.05.019](https://doi.org/10.1016/j.seppur.2007.05.019).
- [19] X. Yan, M. Hou, H. Zhang, F. Jing, P. Ming, and B. Yi, "Performance of PEMFC stack using expanded graphite bipolar plate", *J. Power Sourc.*, vol. 160, pp. 252–257, 2006.
- [20] C. Du, P. Ming, M. Hou, J. Fud, Y. Fuc, X. Luo, Q. Shen, Z. Shao, and B. Yi, "The preparation technique optimization of epoxy/compressed expanded graphite composite bipolar plates for proton exchange membrane fuel cells", *J. Power Sourc.*, vol. 195, pp. 5312–5319, 2010, doi: [10.1016/j.jpowsour.2010.03.005](https://doi.org/10.1016/j.jpowsour.2010.03.005).
- [21] C. Du, *et al.*, "Preparation and properties of thin epoxy/compressed expanded graphite composite bipolar plates for proton exchange membrane fuel cells", *J. Power Sourc.*, vol. 195, pp. 794–800, 2010.

- [22] R. Włodarczyk, Porous carbon materials for elements in low-temperature fuel cells”, *Arch. Metal. and Mater.*, vol. 60, no. 1, pp. 117–120, 2015, doi: [10.1515/amm-2015-0019](https://doi.org/10.1515/amm-2015-0019).
- [23] J. Berdowski, S. Berdowska, and F. Aubry, “Study of properties of expanded graphite-polymer porous composites by acoustic emission method”, *Arch. Metall. Mater.*, vol. 58, no. 4, pp. 1331–1336, 2013, doi: [10.2478/amm-2013-0169](https://doi.org/10.2478/amm-2013-0169).
- [24] A. Berdowska, J. Berdowski, and F. Aubry, “Study of graphite – polymer – turbostratic carbon composites by acoustic emission method at perpendicular geometry”, *Arch. Metall. Mater.*, vol. 63, no. 3, pp. 1287–1293, 2018, doi: [10.24425/123803](https://doi.org/10.24425/123803).
- [25] Z. Ranachowski, *Measurements and analysis of the acoustic emission signal*, Warsaw, IPPT PAN, 1996, [in Polish].
- [26] A. Zakupin, et al., *Acoustic emission*, ed., W. Sikorski, Rijeka, Shanghai, In Tech, 2012, pp. 173–198.
- [27] M. Šofer, J. Cienciala, M. Fusek, P. Pavlíček, and R. Moravec, “Damage analysis of composite CFRP tubes using acoustic emission monitoring and pattern recognition approach”, *Materials*, vol. 14, no. 4, pp. 786, 2021, doi: [10.3390/ma14040786](https://doi.org/10.3390/ma14040786)
- [28] J. Zapała-Sławeta, and G. Świt, “Monitoring of the impact of lithium nitrate on the alkali-aggregate reaction using acoustic emission methods”, *Materials*, vol. 12, no. 1, pp. 20–28, 2019.
- [29] J. Li, F. Beall, and T. Breiner, “Analysis of racking of structural assemblies using acoustic emission”, in *Advances in acoustic emission*, ed., K. Ono, Nevada, USA, Acoustic Emission Working Group, 2007, pp. 202–207.
- [30] G. Świt and J. Zapała-Sławeta, “Application of acoustic emission to monitoring the course of the alkali-silica reaction”, *Bull. Pol. Acad. Sci. Tech. Sci.*, vol. 68, pp. 169–178, 2020, doi: [10.24425/bpasts.2020.131832](https://doi.org/10.24425/bpasts.2020.131832).
- [31] I. Malecki, and J. Ranachowski, *Acoustic emission*, Warsaw, PASCAL, 1994, [in Polish].
- [32] A. Jaroszewska, J. Ranachowski, and F. Rejmund, “Destruction processes and material strength”, ed. J. Ranachowski, Warsaw, IPPT PAN, 1996, pp. 183, [in Polish].
- [33] A. Dode and M. Rao, “Pattern recognition of acoustic emission signals from PZT ceramics”, *NDT.net*, vol. 7, no. 9, 2002.
- [34] M. Raminnea, “Frequency analysis in sandwich higher order plates imposing various boundary conditions”, *Int. J. Hydromechatronics*, vol. 2, no. 1, pp. 63–76, 2019.
- [35] K. Ito and M. Enoki, “Real-time denoising of AE signals by short time Fourier transform and wavelet transform”, in *Advances in acoustic emission*, ed. K. Ono, Nevada, USA, Acoustic Emission Working Group, 2007, pp. 94–99.